Cholinergic chemosensory cells in the trachea regulate breathing

Gabriela Krasteva[a,1], Brendan J. Canning[b], Petra Hartmann[a], Tibor Z. Veres[c], Tamara Papadakis[a], Christian Mühlfeld[a], Kirstin Schliecker[a], Yvonne N. Tallini[d], Armin Braun[c], Holger Hackstein[e], Nelli Baal[e], Eberhard Weihe[f], Burkhard Schütz[f], Michael Kotlikoff[d], Ines Ibanez-Tallon[g], and Wolfgang Kummer[a]

[a]Institute of Anatomy and Cell Biology and [e]Institute for Clinical Immunology and Transfusion Medicine, Justus-Liebig-University, Giessen D-35385, Germany; [b]Johns Hopkins Asthma and Allergy Center, Baltimore, MD 21224; [c]Fraunhofer Institute for Toxicology and Experimental Medicine, Hannover D-30625, Germany; [d]Department of Biomedical Sciences, College of Veterinary Medicine, Ithaca, NY 14853; [f]Institute for Anatomy and Cell Biology, Philipps-University Marburg, D-35037 Marburg, Germany; and [g]Max-Delbrück-Centre for Molecular Medicine, Berlin D-13092, Germany

Edited* by Ewald R. Weibel, University of Bern, Bern, Switzerland, and approved May 2, 2011 (received for review December 23, 2010)

In the epithelium of the lower airways, a cell type of unknown function has been termed "brush cell" because of a distinctive ultrastructural feature, an apical tuft of microvilli. Morphologically similar cells in the nose have been identified as solitary chemosensory cells responding to taste stimuli and triggering trigeminal reflexes. Here we show that brush cells of the mouse trachea express the receptors (Tas2R105, Tas2R108), the downstream signaling molecules (α-gustducin, phospholipase $C_{β2}$) of bitter taste transduction, the synthesis and packaging machinery for acetylcholine, and are addressed by vagal sensory nerve fibers carrying nicotinic acetylcholine receptors. Tracheal application of an nAChR agonist caused a reduction in breathing frequency. Similarly, cycloheximide, a Tas2R108 agonist, evoked a drop in respiratory rate, being sensitive to nicotinic receptor blockade and epithelium removal. This identifies brush cells as cholinergic sensors of the chemical composition of the lower airway luminal microenvironment that are directly linked to the regulation of respiration.

airway sensory innervation | respiratory epithelium | jugular–nodose ganglion | bitter-tasting substances

The so-called "brush cells" of the respiratory epithelium of the lower airways are morphologically defined by an apical tuft of microvilli containing the structural proteins villin and fimbrin (1). Despite some similarities, they are different from solitary neuroendocrine cells of the epithelium that can give rise to small-cell lung carcinoma (2). The function of brush cells in the lower airway epithelium is still unclear. Originally, a resorptive function and hence a role in regulation of the viscosity of the mucous had been postulated (3), whereas recent evidence points toward a chemosensory function (4). Alpha-gustducin and phospholipase $C_{β2}$ (PLC-β2), elements of the bitter and sweet sensing transduction cascade, have been detected in solitary, putative brush cells of the rat trachea (5), and we identified TRPM5, a taste-signaling (sweet, bitter, amino acid) transient receptor potential cation-channel in rat and mouse tracheal brush cells (6). Morphologically similar cells in the mouse nasal epithelium express α-gustducin (7) and respond to bitter stimuli, and their activation evokes respiratory reflexes via afferent neurons of the trigeminal nerves (8, 9). Analyzing a mouse strain expressing enhanced GFP (eGFP) under the control of the promoter of the acetylcholine synthesizing enzyme, choline acetyltransferase (ChAT), solitary ChAT-eGFP$^+$ cells were located in the tracheal epithelium that did not express a marker protein of solitary neuroendocrine cells (10). This led us to the hypothesis that brush cells of the lower airway epithelium are solitary chemosensory cells that sense the chemical composition of the airway lining fluid and transmit this information to sensory nerve endings via cholinergic transmission.

Results

Tracheal Brush Cells Are Cholinergic. We observed solitary flask-shaped or triangular eGFP$^+$ cells in the tracheal epithelium of two independently generated mouse strains with knockin of eGFP within a BAC spanning the ChAT locus (10, 11). The average number of these cells in a mouse trachea was 6242 ± 989 with approximately twice as many cells located above noncartilagenous regions (4,065 ± 640 cells) than in epithelial stretches overlaying cartilage rings (2,177 ± 550 cells) (Fig. S1). Only a few of such cells were located in the main extrapulmonary bronchi, and they occurred only in exceptional cases distal to the lung hilus. Immunohistochemistry demonstrated expression of villin in these cells, a marker protein of brush cells (Fig. 1 *A* and *A′*), and ultrastructural eGFP immunohistochemistry revealed their brush cell morphology (Fig. 1*B*). The cholinergic nature of the ChAT-eGFP$^+$ brush cells was further documented by their immunoreactivity for the vesicular acetylcholine transporter (VAChT), a membrane protein of cholinergic vesicles (12) (Fig. 1 *C* and *C′*) and observation of VAChT-IR in villin-positive cells in wild-type tracheas (not shown). Although all ChAT-eGFP$^+$ cells were immunoreactive to villin, a small fraction (17%; 164 cells/4 mice) of villin-positive cells did not exhibit eGFP (Fig. 1*D*), even when visualization of eGFP was enhanced by eGFP immunolabeling (Fig. 1*E*), strongly suggesting heterogeneity of tracheal brush cells.

Cholinergic Brush Cells Express a Bitter Taste Transduction System. Detection of bitter substances is achieved by a variety of taste receptors of the T2R family that are coupled to the G protein, α-gustducin. Their stimulation leads to activation of PLC-β2 and, subsequently, to opening of TRPM5 channels (13–15). We previously identified TRPM5 in tracheal brush cells (6). Here, we detected α-gustducin immunoreactivity and PLC-β2 immunoreactivity in cholinergic (ChAT-eGFP$^+$) brush cells (Fig. 2 *A*–*B′*). In this respect, tracheal cholinergic brush cells differ from cholinergic cells in the taste buds of the circumvallate papillae (16), which we found to be largely separate from α-gustducin- and PLC-β2-immunoreactive taste cells (Fig. 2 *C* and *D*).

In the absence of specific antibodies against murine T2R subtypes, we investigated their expression by RT-PCR. Of the 35 known mouse T2Rs, ligands are identified for T2R105 (cycloheximide) and T2R108 (denatonium) (17, 18). For both, mRNA was detected in abraded tracheal epithelium, along with α-gustducin mRNA and PLC-β2 mRNA (Fig. 2*E*). ChAT-eGFP$^+$ cells were then purified by FACS from freshly dissociated epithelial cells. RT-

Author contributions: G.K., B.J.C., and W.K. designed research; G.K., P.H., T.Z.V., T.P., C.M., K.S., and W.K. performed research; Y.N.T., A.B., H.H., N.B., E.W., B.S., M.K., and I.I.-T. contributed new reagents/analytic tools; G.K., B.J.C., P.H., and W.K. analyzed data; and G.K., B.J.C., and W.K. wrote the paper.

The authors declare no conflict of interest.

*This Direct Submission article had a prearranged editor.

[1]To whom correspondence should be addressed. E-mail: Gabriela.Krasteva@anatomie.med.uni-giessen.de.

This article contains supporting information online at www.pnas.org/lookup/suppl/doi:10.1073/pnas.1019418108/-/DCSupplemental.

www.pnas.org/cgi/doi/10.1073/pnas.1019418108

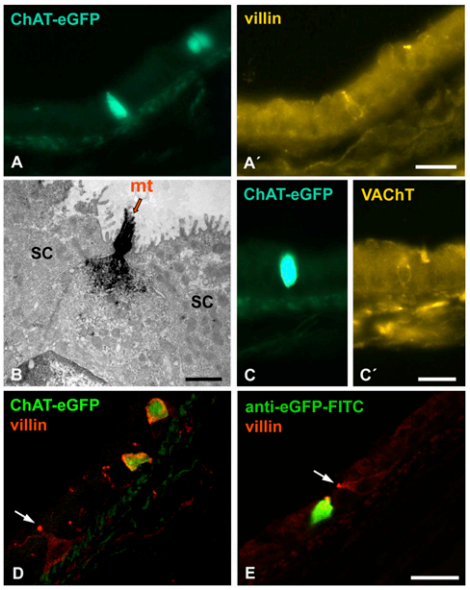

Fig. 1. Tracheal ChAT-eGFP cells are cholinergic brush cells. (*A* and *A′*) ChAT-eGFP–expressing cells are immunoreactive for villin, a structural protein of microvilli of brush cells. (Scale bar, 20 μm.) (*B*) Ultrastructural preembedding anti-eGFP immunohistochemistry. ChAT-eGFP cell with micovilli tuft (mt) typical for brush cells, flanked by secretory cells (SC). (Scale bar, 1 μm.) (*C* and *C′*) Epifluorescence. ChAT-eGFP–expressing cell is immunoreactive for the vesicular ACh transporter (VAChT), further validating its cholinergic nature. (Scale bar, 20 μm.) (*D* and *E*) CLSM analysis, merged images. In addition to double-labeled cells, a villin-positive cell (arrow) with triangular shape is negative for ChAT (*D*), also when the eGFP signal is enhanced by immunolabeling (*E*). (Scale bar, 20 μm.)

PCR analysis of the purified fraction validated eGFP expression, confirming that the cells of interest had been harvested, whereas expression of α-tubulin (marker for ciliated cells), protein gene product (PGP) 9.5 (neuroendocrine cell marker), and myosin heavy chain (smooth muscle cells) was not detectable (Fig. 2*F*). These purified cells expressed the full range of the bitter taste transduction system from the receptor to the second messenger generating enzyme (i.e., T2R105, T2R108, α-gustducin, and PLC-β2) (Fig. 2*F* and Fig. S2).

Cholinergic Tracheal Brush Cells Are Connected to Cholinoceptive Sensory Nerve Fibers. Tracheal whole-mount preparations from $ChAT^{BAC}$-eGFP mice were triple-stained for eGFP (to enhance fluorescence of ChAT-eGFP$^+$ cells), PGP 9.5 (to visualize both nerve fibers and solitary neuroendocrine cells), and calcitonin gene-related peptide (CGRP; to visualize sub- and intraepithelial sensory C-fibers). As previously deduced from tissue sections, ChAT-eGFP$^+$ cells and neuroendocrine cells represent separate entities (Fig. 3). Both cell types, however, receive contacts from CGRP-positive (5.8% for brush cells and 5.9% for neuroendocrine cells) and nonpeptidergic (PGP 9.5-positive, CGRP-negative; 21.7% for brush cells and 21% for neuroendocrine cells) nerve fibers. Confocal analysis of immunolabeled cross-sections confirmed the whole-mount data (Fig. S3 *A–B′*). Interestingly, expression of the presynaptic protein SNAP 25 was not detected in brush cells (Fig. S3 *C–E*). We next set out to determine whether such nerve fibers express cholinergic receptors and are indeed sensory. Tracheal sensory nerve fibers originate mainly from cell bodies located in vagal sensory ganglia (19–21), where the α3- and β4-subunits are the most widely expressed subunits of nicotinic acetylcholine receptors (nAChR) (22). Hence, we investigated the tracheal mucosa and vagal sensory ganglia in BAC transgenic mice with eGFP driven by the nAChR α3β4α5 cluster Tg(Chrna3-EGFP) (23). Sensory neurons expressing eGFP fluorescence in this transgenic line indeed carry functional nAChRs: they respond to nicotine with a sharp increase in cytosolic calcium concentration (Fig. S4). Intraepithelial nAChR-positive nerve fibers were colabeled for CGRP (Fig. 4 *B–B″*) and seemed to establish close contacts to villin-positive (brush) cells (Fig. 4 *A–A″*). The sensory vagal origin of such nerve fibers was confirmed by retrograde neuronal labeling using Fast Blue instillation in the airways. Six percent of all retrogradely labeled neurons in the jugular–nodose complex (n = 1,878 Fast Blue$^+$ neurons from four animals) exhibited an nAChR-eGFP$^+$/CGRP$^+$ phenotype (Fig. 4 *C–C″*), another 2% were nAChR-eGFP$^+$ without additional CGRP immunolabeling, and 9% were solely CGRP immunoreactive. Hence, cholinergic brush cells contact a population of peptidergic (CGRP) cholinoceptive vagal sensory neurons.

Mucosal Application of a Bitter Substance Elicits a Cholinergically Driven Respiratory Reflex. The morphological studies summarized above suggest that tracheal cholinergic brush cells detect bitter substances in the airway lining fluid and transmit this information through the release of acetylcholine, which in turn activates nAChRs on adjacent sensory nerve fibers, resulting in action potentials and ultimately respiratory reflexes. To address this hypothesis directly, a method was established that allows monitoring respiratory efforts in a freely breathing mouse while perfusing the mucosal surface of the upper cervical trachea with test substances (Fig. S5). Capsaicin, a known activator of afferent C-fibers (24, 25) and here used as a test substance to validate the system, elicited sharp changes in respiration, accompanied by abrupt decreases in respiratory rate ("respiratory events") (Fig. 5*A*). This reflex response was substance specific and not caused by perfusion with buffer alone (Fig. 5*B* and Fig. S6). A nicotinic agonist, 1,1-dimethyl-4-phenylpiperazinium iodide (DMPP), did not elicit respiratory events of the capsaicin-type but led to a long-lasting drop in respiratory rate with late onset (Fig. 5*C*). A comparable pattern was observed in response to 10 and 100 μM cycloheximide, a bitter substance and T2R105 agonist (Fig. 5*D* and Fig. S6). We chose this bitter substance instead of denatonium, a T2R108 agonist, because cycloheximide did not directly affect other respiratory epithelial cells (Fig. S7), in contrast to denatonium, which increases ciliary beat frequency in differentiated cultured human ciliated cells (26).

The nAChR antagonist mecamylamine, superfused directly over the tracheal mucosa, inhibited the respiratory reflexes evoked by tracheal cycloheximide but not those evoked by capsaicin (Fig. 5 *E* and *E′*), demonstrating involvement of cholinergic transmission in the cycloheximide evoked responses. Abrading the airway epithelium also prevented the responses evoked by cycloheximide in three out of four experiments, even though complete denudation was never achieved, as evidenced by postmortem visualizaton of airway epithelial cells and the underlying sensory nerve terminals using FM1-43 (Fig. 5 *D* and *D″*), and by the unaffected response to capsaicin. Indeed, especially large stretches of epithelium were left intact in the trachea of the one animal that still responded to cycloheximide after mechanical abrasion (Fig. 5*D′*).

Discussion

In the respiratory tract, direct proof for bitter taste sensing has been provided for solitary chemosensory cells of the nasal cavity, the classic site for probing the incoming airstream, involving as-yet unidentified neurotransmitters (8, 9). In the nose, bitter compounds of bacterial origin, such as acyl-homoserine lactones, trigger trigeminally mediated transient respiratory depression (9). This reflex is considered protective by avoiding further inhalation of bacteria, and the anticipated simultaneous release of neuropeptides in the mucosa may trigger an inflammatory response before the bacteria grow to population densities capable of forming destructive biofilms (9). Similarly, ChAT-expressing solitary che-

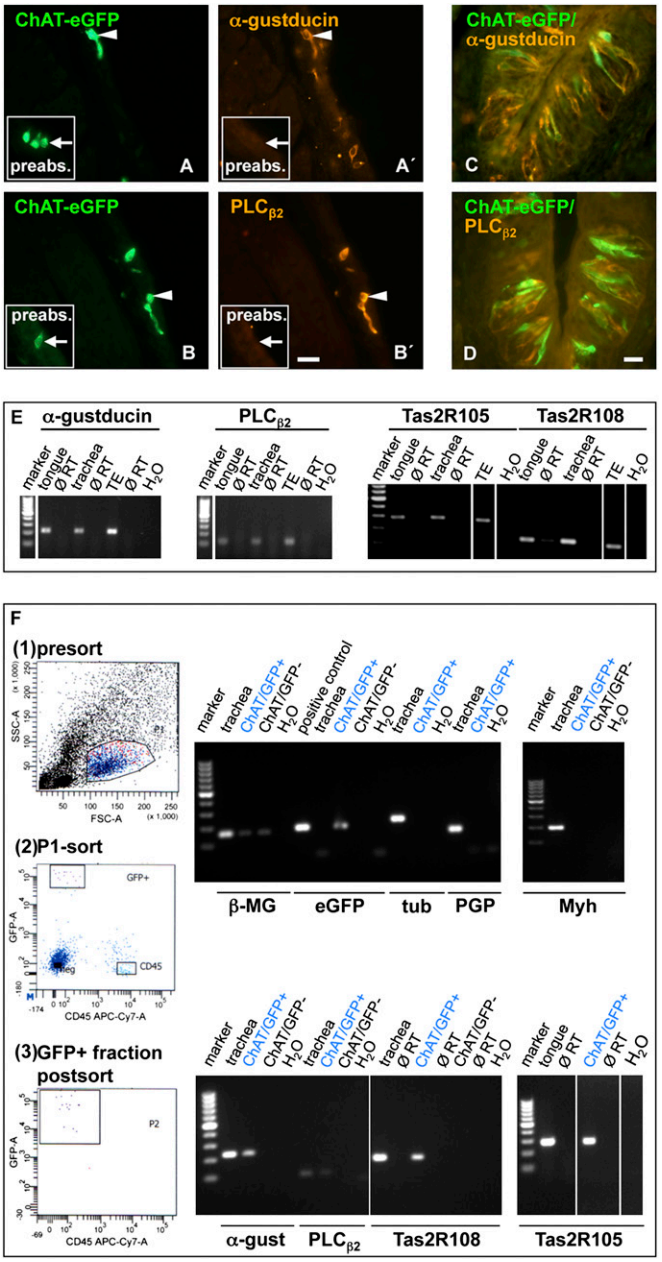

Fig. 2. Tracheal ChAT-eGFP–expressing cells are chemosensory. (*A–D*) Immunohistochemistry. (*A* and *B*) Trachea. ChAT-eGFP cells (arrowheads) are positive for α-gustducin (*A* and *A′*) and PLC-β2 (*B* and *B′*). *Inset:* Preabsorbtion (preabs.) of the antibodies with the corresponding peptides abolishes immunoreactivity for α-gustducin and PLC-β2 in ChAT-eGFP cells (arrows). (*C* and *D*) Tongue, merged images. In the vallate papilla used as a positive control for antibody specificities, no colocalization was found between α-gustducin (*C*) and PLC-β2 (*D*) and ChAT-eGFP, respectively. (Scale bar, 20 μm.) (*E*) RT-PCR. Alpha-gustducin, PLC-β2, and bitter taste receptors 105 (Tas2R105) and 108 (Tas2R108) are expressed in whole-trachea homogenate and abraded tracheal epithelial cells (TE); tongue served as positive control. Negative controls included samples in absence of reverse transcriptase (Ø RT) and without template (H_2O). Marker = 100 base pairs. (*F*) RT-PCR of ChAT-eGFP cells isolated by FACS. (*1*) FACS analysis of isolated tracheal cells. P1 represents a subgroup of cells that includes the population of ChAT-eGFP expressing cells. (*2*) Representative dot plot showing gating on the ChAT-eGFP cells (GFP^+) and $CD45^+$ cells, and nonfluorescent cells (neg), used for sorting. (*3*) Representative dot plot of postsort analysis. Highly purified fraction of ChAT-eGFP cells after FACS sorting (97.5%) was collected and processed in RT-PCR experiments (*Right*). Tracheal homogenate was applied as a positive control for all investigated genes except eGFP, for which we used $eGFP^+$ tissue biopsy (control DNA). mRNA for eGFP, α-gustducin, PLC-β2, for the cycloheximide receptor Tas2R105, and the denatonium receptor Tas2R108 is detected in the $ChAT/eGFP^+$ fraction; respective lanes are highlighted by the blue label. Contamination of this cell fraction with other cell types is excluded by the lack of mRNA for tubulin (tub), a marker for ciliated cells, for protein gene product 9.5 (PGP), a marker for neuroendocrine cells, and for myosin heavy chain (Myh), a marker for smooth muscle cells. Corresponding cell numbers of the $ChAT/eGFP^+$ fraction do not express taste-related genes. β-Microglobulin (β-MG) served as housekeeping gene to control for mRNA quality and PCR efficiency. All control reactions including samples in absence of reverse transcriptase (Ø RT) and without template (H_2O) were negative.

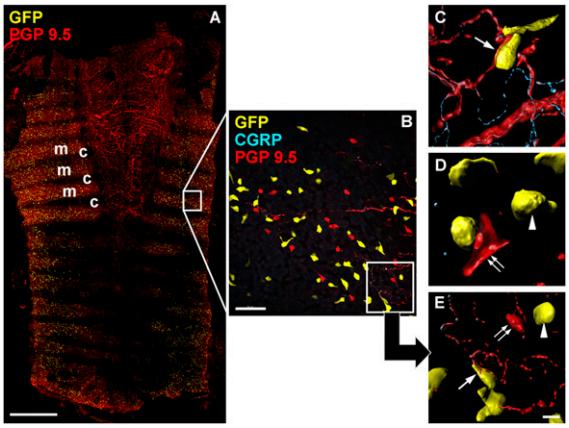

Fig. 3. Tracheal ChAT-eGFP brush cells are contacted by intraepithelial nerve fibers. Whole-mount immunohistochemistry, CLSM, 3D analysis. (*A*) ChAT-eGFP cells (yellow) are predominantly localized at the ligamentous parts (m) between the cartilage rings (c). (Scale bar, 1,000 μm.) (*B*) magnified region from *A*. A fine network of $PGP\ 9.5^+$ fibers (red), partly colocalizing with CGRP immunoreactivity (blue), extends within and underneath the epithelium. ChAT-eGFP cells (yellow) are distinct from neuroendocrine cells ($PGP\ 9.5^+$, red). (Scale bar, 50 μm.) (*C* and *D*) $ChAT\text{-}GFP^+$ epithelial cells are seen in direct contact with $PGP\ 9.5^+/CGRP^+$ fibers (arrow in *E*; magnified *Inset* from *B*), with $PGP\ 9.5^+/CGRP^-$ fibers (arrow in *C*), or lack direct contact to nerve fibers (arrowheads in *D* and *E*). Neuroendocrine cells ($PGP\ 9.5^+$, doubled arrows) are also seen with and without nerve fiber contacts. (Scale bar, 10 μm.)

mosensory cells at the entrance duct of the vomeronasal organ regulate access of chemical fluids into this pheromone sensing organ (27). For the lower airways, morphological criteria (28) and immunohistochemistry for proteins of the taste signaling cascade downstream of the actual receptor protein (5, 6) suggested that brush cells are solitary chemosensory cells monitoring the composition of the airway lining fluid (28, 29). Recently, expression of Tas2Rs was shown in the rat airways (30). Still, the exact cell type expressing the actual taste receptors, the stimuli that excite them, the responses evoked upon stimulation, and the messengers mediating these responses remained unknown. Here we demonstrate that brush cells of the tracheal epithelium are solitary chemosensory cells that sense bitter compounds in the airway lining fluid, transmit this information to sensory nerve endings via cholinergic transmission, and thereby initiate an aversive reflex (i.e., reduction of respiratory rate). This reflex differentiates this system from purely local or "cell autonomous" responses to taste stimuli like those being described for ciliated cells cultured from human airways that respond to bitter stimuli with increases in ciliary beat frequency (26). Recently, an aerosolized administration of bitter substances was reported to relax the airways in a mouse model of allergic inflammation (31). Still, it remains unclear how the bitter substances access the smooth muscle layer in vivo and whether a possible mechanism is an activation of tracheal chemosensory brush cells, which secondarily activate the airway smooth muscle.

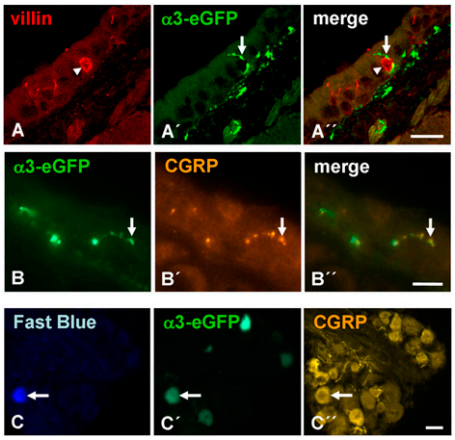

Fig. 4. Brush cells have contact to vagal cholinoceptive peptidergic sensory neurons. (*A–C*) Samples taken from Tg(Chrna3-EGFP) BAC transgenic mice. (*A*) An intraepithelial nerve fiber expressing eGFP in transgenic nAChR-eGFP mice (arrow) attaches to a villin$^+$ brush cell (arrowhead). (*B* and *C*) Colocalization of CGRP and nAChR-eGFP expression can be observed in intraepithelial terminals (*B*) and neurons in the vagal jugular–nodose complex, which are retrogradely labeled with Fast Blue from the airways (*C*). (Scale bars, 20 μm.)

Indeed, there are direct contacts between tracheal brush cells and sensory nerve fibers, as demonstrated in the present confocal and in earlier electron microscopic studies (28). Sensory nerve fibers approaching tracheal cholinergic chemosensory cells are of at least two types: peptidergic (CGRP positive) and nonpeptidergic. Both types were also identified by retrograde neuronal tracing, and a subset of each type also expressed nAChRs. It is currently unclear which of these afferent nerve subtypes triggers the respiratory reflexes evoked by nAChR stimulation. As for the CGRP-positive population, however, it is known that acetylcholine and nicotine evoke direct release of neuropeptide from the peripheral terminal in the rat trachea (32), which causes local neurogenic inflammation involving plasma extravasation and activation of the innate immune system (33). Hence, innervated cholinergic chemosensory cells are likely to trigger local defensive reflexes in addition to centrally mediated respiratory and likely autonomic reflexes.

We found that the majority of cholinergic chemosensory cells do not receive direct innervation, in line with the recent observations of Tizzano et al. (9), showing that tracheal TRPM5-positive cells are less innervated than those of the nasal cavity. Acetylcholine released from such noninnervated chemosensory cells may exert paracrine actions, such as local stimulation of secretion (34). Indeed, administration of bitter compounds provokes secretion of airway surface liquid in the rat trachea (35), but the link between chemoreception and secretion remains to be determined. Notably, cycloheximide doses that effectively triggered reflex initiation had no impact on overall cilia-driven particle transport on the tracheal surface, whereas, in the same experimental setup, particle transport speed is doubled in response to pharmacological stimulation of muscarinic cholinergic receptors (36). Thus, at least under the present conditions, cholinergic effects triggered by cycloheximide are restricted to the immediate surrounding of the cholinergic cells and do no spread over the entire mucosal surface.

In conclusion, we propose a concept of breathing control involving brush cells as cholinergic sensors of the chemical composition of the lower airway luminal microenvironment that are directly linked to vagal regulation of respiration.

Materials and Methods

Immunohistochemistry. Information about animals, tissue preparation, antibodies, and peptides used in the study is given in *SI Materials and Methods* and Table S1. Cryosections (10 μm) were incubated for 1 h with blocking solution containing 50% horse serum, followed by an overnight incubation with the primary antisera. Combinations were as follows: chicken anti-eGFP/rabbit anti-PGP 9.5, chicken anti-eGFP/rabbit anti-CGRP, chicken anti-eGFP/rabbit anti-villin, chicken anti-eGFP/rabbit anti-α-gustducin, and chicken anti-eGFP/rabbit anti-PLC-β2. Here, anti-eGFP staining was first accomplished, and then immunolabeling for the second antigen was performed. Slides were evaluated with an epifluorescence microscope (Zeiss) and with a confocal laser scanning microscope (CLSM) (Leica-TCS SP2 AOBS; Leica).

Preembedding Immunohistochemistry and Electron Microscopy. Specimen preparation and analyses were performed as described previously (37). *SI Materials and Methods* provides a detailed description of experimental procedures.

Whole-Mount Immunostaining and Confocal Analysis. The antibody staining was performed as previously described (37). Image stacks for the quantitative analysis were scanned with an XYZ-resolution of 1,024 × 1,024 × 53, with dimensions of 318.2 μm × 318.2 μm × 30 μm, respectively, starting from the luminal side of the tracheal epithelium. Four image stacks (two at the proximal and two at the distal halves) were taken of each of the three tracheas. Image stacks were analyzed using Imaris 6.2.1. (Bitplane). In each dataset, 10 GFP$^+$ epithelial cells (altogether n = 120) were randomly selected and manually examined to determine whether they had direct contact to PGP 9.5$^+$ and/or CGRP$^+$ nerve fibers and to PGP 9.5$^+$ epithelial cells. Subsequently, 10 PGP 9.5$^+$ epithelial cells were examined in the same fashion.

Tracing of Trachea and Lung Afferents. Tracing of airway afferents was performed on adult Tg(Chrna3-EGFP) mice (n = 14) from either sex. The experiments were conducted in accordance with the European Communities Council Directive of November 25, 1986 (86/609/EEC). Briefly, animals were anesthetized, and 2.5–2.7 μL of tracer Fast Blue (Polyscience) were injected into the tracheal lumen (detailed description in *SI Materials and Methods*). The animals were allowed to recover and were killed at the fourth postoperative day. Spinal cord at segmental levels C1–C5, the jugular–nodose complex, and thoracic viscera en bloc were dissected and further processed for immunohistochemisty. Sections were labeled for CGRP/Cy3 and NF 68/Cy5, and the neurochemical characteristics from ≈500 neurons from each ganglion labeled by Fast Blue were recorded.

Fluorescence-Activated Cell Sorting. A pure population of brush cells was obtained by FACS analysis. Description of the isolation of tracheal cells is given in *SI Materials and Methods*. Leukocytes were stained with an APS/Cy7-conjugated anti-mouse CD-45 antibody (1:125; BioLegend). Fluorescence compensation settings were established using BD CompBead Plus Anti-Mouse Ig-κ beads. FACS was performed using a BD FACSAria II cell sorter. Sorting gates were set on the low side scatter (SSC)/eGFP$^+$ cell population. Cell debris was excluded by appropriate gate setting. Cells were sorted in HBSS buffer and kept on ice until processing with RT-PCR experiments. Data acquisition and analysis were performed using the BD FACSDiva Software package (all from BD Biosciences PharMingen).

RT-PCR with Cells Sorted by FACS/Single-Cell RT-PCR. First-strand cDNA was synthesized from sorted ChAT-eGFP$^+$ cells (400 hits) or from single eGFP-fluorescent cells by using the Super-Script III CellsDirect cDNA Synthesis System (Invitrogen) according to the manufacturer's recommendations. Three microliters of each sample (cDNA, Ø RT, or H_2O control) was used for PCR amplification (conditions are given in *SI Materials and Methods*) of mouse β-actin, eGFP, α-gustducin, PLC-β2, Tas2R105 and 108, tubulin, PGP 9.5, and Myh by the HotStar Taq Poymerase Kit (Qiagen) according to the manufacturer's recommendations (primers listed in Table S2). Products were visualized in ethidium bromide-stained 1.5% agarose gels.

Monitoring of Respiratory Function. A detailed diagram and description of the preparation used to monitor respiratory reflexes is provided in Fig. S4. Mice were anesthetized with urethane (1.5 g/kg i.p.). First, respiratory function at baseline was assessed during 5-min continuous perfusion of the tracheal mucosa with Krebs buffer alone or in the presence of the nAChR antagonist mecamylamine (10^{-4} M). Mice with intact epithelium or after mechanical abrasion of the epithelium were challenged with solutions containing either DMPP (10^{-5} M) or cycloheximide (10^{-4} M) for the subsequent 5 min. Vehicle control experiments were carried out in separate animals. For studying the kinetic of the responses, mice with intact epithelium were challenged after achievement of the baseline for an additional 5 min with vehicle and subsequently with 10^{-5} M cycloheximide. In experiments performed with DMPP, atropine was added to all solutions.

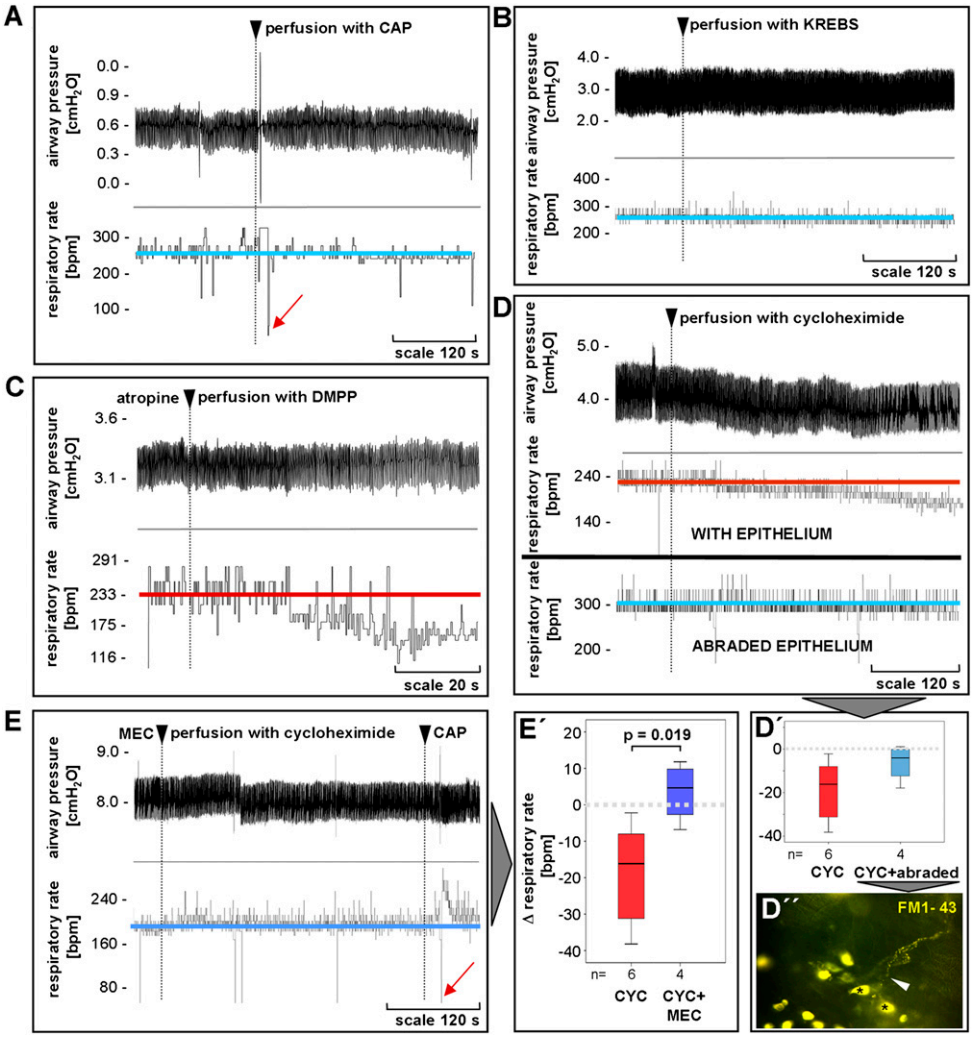

Fig. 5. The bitter substance cycloheximide elicits an epithelium-dependent depressive respiratory reflex involving nicotinic transmission. All data from anesthetized, spontaneously breathing mice, representative traces depicted in *A–E*. (*A* and *B*) Model validation. Challenge of the trachea with capsaicin (CAP) evokes a rapid and transient change in respiration (arrow) resembling a single augmented breath (*A*), which is not seen after perfusion with Krebs buffer (baseline = blue line). (*C*) Perfusion with the nicotinic receptor agonist DMPP (10 μM) in the presence of atropine leads to a dramatic drop in the respiratory rate. (*D* and *E*) Cycloheximide (100 μM), a bitter substance that has affinity for Tas2R105, also causes a drop in the respiratory rate, which is completely abrogated by the nicotinic antagonist mecamylamine (MEC, 10 μM). The response to 10 μM capsaicin (CAP), however, persisted under nicotinic blockade (arrow = augmented breath). Mechanical disruption of the epithelium (*D*, *Lower*) abolishes the cycloheximide (CYC) effect in three out of four animals (box plot, *D′*). (*D″*) Intravital fluorescence staining of the trachea with FM1-43 at the end of the experiment in which the animal still responded to cycloheximide revealed incomplete abrasion of the epithelial layer, and single epithelial cells (asterisks) are still contacted by capsaicin-sensitive nerve fibers (arrowhead). (*D′* and *E′*) Statistical analyses of experiments shown representatively in *E* and *D*. Box plots: percentiles 0, 25, median, 75, and 100 (Mann-Whitney test, $P \leq 0.05$ is considered significant).

To assess viability of the preparation at the end of each experiment, tracheae were challenged topically with capsaicin (10^{-5} M). At the end of all experiments, mice were killed by cervical dislocation. All reagents were purchased from Sigma-Aldrich.

A modification of the method by Meyers et al. (38) was used to label capsaicin-sensitive nerve terminals in the airways and to assess epithelial integrity postmortem. Digital images of trachea were captured using a JenOptik cooled CCD digital camera.

Statistical Analysis. We used an unpaired experimental design for all of the studies described above. Respiratory rate under nonstimulatory conditions was set as baseline. Changes in respiratory rate were calculated. Differences among group means were assessed by Kruskal-Wallis test, followed by Mann-Whitney test. A P value ≤ 0.05 was considered significant.

ACKNOWLEDGMENTS. We thank Karola Michael for expert technical help with the figures, and Emma Spies for excellent technical assistance. B.J.C. was supported by National Institutes of Health Grant HL083192. This work was supported by a Young Investigator Grant from the Medical Faculty of the Justus-Liebig-University Giessen, Germany, Universities of Giessen and Marburg Lung Center, von Behring-Röntgen-Stiftung, and the Deutsche Forschungsgemeinschaft.

1. Reid L, et al. (2005) The mysterious pulmonary brush cell: A cell in search of a function. *Am J Respir Crit Care Med* 172:136–139.
2. Sbarbati A, Osculati F (2005) The taste cell-related diffuse chemosensory system. *Prog Neurobiol* 75:295–307.
3. Rhodin J, Dalhamn T (1956) Electron microscopy of the tracheal ciliated mucosa in rat. *Z Zellforsch Mikrosk Anat* 44:345–412.
4. Sbarbati A, Bramanti P, Benati D, Merigo F (2010) The diffuse chemosensory system: Exploring the iceberg toward the definition of functional roles. *Prog Neurobiol* 91:77–89.
5. Merigo F, Benati D, Tizzano M, Osculati F, Sbarbati A (2005) α-Gustducin immunoreactivity in the airways. *Cell Tissue Res* 319:211–219.
6. Kaske S, et al. (2007) TRPM5, a taste-signaling transient receptor potential ion-channel, is a ubiquitous signaling component in chemosensory cells. *BMC Neurosci* 8:49.

7. Zancanaro C, Caretta CM, Merigo F, Cavaggioni A, Osculati F (1999) alpha-Gustducin expression in the vomeronasal organ of the mouse. *Eur J Neurosci* 11:4473–4475.
8. Finger TE, et al. (2003) Solitary chemoreceptor cells in the nasal cavity serve as sentinels of respiration. *Proc Natl Acad Sci USA* 100:8981–8986.
9. Tizzano M, et al. (2010) Nasal chemosensory cells use bitter taste signaling to detect irritants and bacterial signals. *Proc Natl Acad Sci USA* 107:3210–3215.
10. Tallini YN, et al. (2006) BAC transgenic mice express enhanced green fluorescent protein in central and peripheral cholinergic neurons. *Physiol Genomics* 27:391–397.
11. von Engelhardt J, Eliava M, Meyer AH, Rozov A, Monyer H (2007) Functional characterization of intrinsic cholinergic interneurons in the cortex. *J Neurosci* 27: 5633–5642.
12. Parsons SM (2000) Transport mechanisms in acetylcholine and monoamine storage. *FASEB J* 14:2423–2434.
13. Liman ER (2007) TRPM5 and taste transduction. *Handb Exp Pharmacol* 179:287–298.
14. Zhang Z, Zhao Z, Margolskee R, Liman E (2007) The transduction channel TRPM5 is gated by intracellular calcium in taste cells. *J Neurosci* 27:5777–5786.
15. Roper SD (2006) Cell communication in taste buds. *Cell Mol Life Sci* 63:1494–1500.
16. Ogura T, et al. (2007) Immuno-localization of vesicular acetylcholine transporter in mouse taste cells and adjacent nerve fibers: indication of acetylcholine release. *Cell Tissue Res* 330:17–28.
17. Chandrashekar J, et al. (2000) T2Rs function as bitter taste receptors. *Cell* 100: 703–711.
18. Bachmanov AA, Beauchamp GK (2007) Taste receptor genes. *Annu Rev Nutr* 27: 389–414.
19. Kummer W, Fischer A, Kurkowski R, Heym C (1992) The sensory and sympathetic innervation of guinea-pig lung and trachea as studied by retrograde neuronal tracing and double-labeling immunohistochemistry. *Neuroscience* 49:715–737.
20. Undem BJ, et al. (2004) Subtypes of vagal afferent C-fibres in guinea-pig lungs. *J Physiol* 556:905–917.
21. Mazzone SB, et al. (2009) Selective expression of a sodium pump isozyme by cough receptors and evidence for its essential role in regulating cough. *J Neurosci* 29: 13662–13671.
22. Mao D, Yasuda RP, Fan H, Wolfe BB, Kellar KJ (2006) Heterogeneity of nicotinic cholinergic receptors in rat superior cervical and nodose Ganglia. *Mol Pharmacol* 70: 1693–1699.
23. Gong S, et al. (2003) A gene expression atlas of the central nervous system based on bacterial artificial chromosomes. *Nature* 425:917–925.
24. Caterina MJ, et al. (2000) Impaired nociception and pain sensation in mice lacking the capsaicin receptor. *Science* 288:306–313.
25. Davis JB, et al. (2000) Vanilloid receptor-1 is essential for inflammatory thermal hyperalgesia. *Nature* 405:183–187.
26. Shah AS, Ben-Shahar Y, Moninger TO, Kline JN, Welsh MJ (2009) Motile cilia of human airway epithelia are chemosensory. *Science* 325:1131–1134.
27. Ogura T, Krosnowski K, Zhang L, Bekkerman M, Lin W (2010) Chemoreception regulates chemical access to mouse vomeronasal organ: role of solitary chemosensory cells. *PLoS ONE* 5:e11924.
28. Luciano L, Reale E, Ruska H (1968) On a "chemoreceptive" sensory cell in the tachea of the rat. *Z Zellforsch Mikrosk Anat* 85:350–375 (in German).
29. Osculati F, et al. (2007) The solitary chemosensory cells and the diffuse chemosensory system of the airway. *Eur J Histochem* 51(Suppl 1):65–72.
30. Tizzano M, Cristofoletti M, Sbarbati A, Finger TE (2011) Expression of taste receptors in solitary chemosensory cells of rodent airways. *BMC Pulm Med* 11:3.
31. Deshpande DA, et al. (2010) Bitter taste receptors on airway smooth muscle bronchodilate by localized calcium signaling and reverse obstruction. *Nat Med* 16: 1299–1304.
32. Jinno S, Hua XY, Yaksh TL (1994) Nicotine and acetylcholine induce release of calcitonin gene-related peptide from rat trachea. *J Appl Physiol* 76:1651–1656.
33. Lundberg JM (1995) Tachykinins, sensory nerves, and asthma—an overview. *Can J Physiol Pharmacol* 73:908–914.
34. Racké K, Matthiesen S (2004) The airway cholinergic system: Physiology and pharmacology. *Pulm Pharmacol Ther* 17:181–198.
35. Boschi F, Nicolato E, Benati D, Marzola P, Sbarbati A (2008) Drug targeting of airway surface liquid: A pharmacological MRI approach. *Biomed Pharmacother* 62:410–419.
36. Klein MK, et al. (2009) Muscarinic receptor subtypes in cilia-driven transport and airway epithelial development. *Eur Respir J* 33:1113–1121.
37. Veres TZ, et al. (2009) Dendritic cell-nerve clusters are sites of T cell proliferation in allergic airway inflammation. *Am J Pathol* 174:808–817.
38. Meyers JR, et al. (2003) Lighting up the senses: FM1-43 loading of sensory cells through nonselective ion channels. *J Neurosci* 23:4054–4065.